# Elongation of Triplet Lifetime Caused by Intramolecular Energy Hopping in Diphenylanthracene Dyads Oriented to Undergo Efficient Triplet–Triplet Annihilation Upconversion

Masaya Kanoh,[1] Yasunori Matsui,[1,2,*] Kiyomasa Honda,[1] Yuto Kokita,[1] Takuya Ogaki,[1,2] Eisuke Ohta,[1,2] and Hiroshi Ikeda[1,2 *]

[1]Department of Applied Chemistry, Graduate School of Engineering, Osaka Prefecture University, 1-1 Gakuen-cho, Nakaku, Sakai, Osaka 599-8531, Japan

[2]The Research Institute for Molecular Electronic Devices (RIMED), Osaka Prefecture University, 1-1 Gakuen-cho, Nakaku, Sakai, Osaka 599-8531, Japan

KEYWORDS: Upconversion, Triplet–Triplet Annihilation, Transient Absorption Spectroscopy, Triplet Lifetime

**ABSTRACT:** Triplet–triplet annihilation (TTA)-assisted photon upconversion (TTA-UC) in three dyads (DPA–Cn–DPA), comprised of two diphenylanthracene (DPA) moieties connected by nonconjugated C1, C2, and C3 linkages (Cn), has been investigated. The performance of these dyads as energy acceptors in the presence of the energy donor platinum octaethylporphyrin are characterized by longer triplet lifetimes ($\tau_T$) and different TTA rate constants than those of the parent DPA. The larger $\tau_T$ of the linked systems, caused by "Intramolecular Energy Hopping" in the triplet dyad $^3$DPA*–Cn–DPA, results in a low threshold intensity, a key characteristic of efficient TTA-UC.

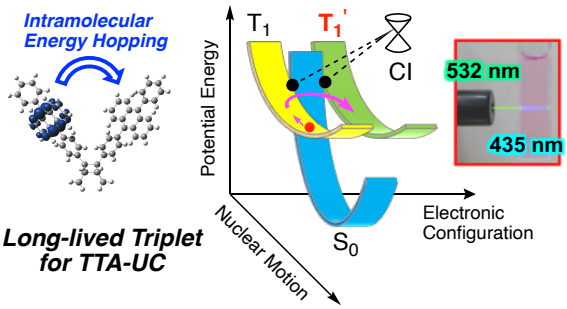


## INTRODUCTION

Triplet–triplet annihilation (TTA)-upconversion (UC),[1,2] a photophysical phenomenon in which long-wavelength light is converted to short-wavelength light of various wavelengths,[3–6] is a promising approach to the efficient use of the sunlight.[7,8] The system comprised of platinum 2,3,7,8,12,13,17,18-octaethylporphyrin (PtOEP) and 9,10-diphenylanthracene (DPA) as a respective energy donor (D) and energy acceptor (A), is a representative of those undergoing TTA-UC. In a conventional TTA-UC mechanism (Fig. 1), an excitation ($h\nu_{EX}$) of D by using a low-energy photon followed by intersystem crossing (ISC) gives a triplet excited state of D ($^3$D*). The succeeding energy transfer (ET) from $^3$D* to A affords $^3$A*. A bimolecular TTA of two $^3$A* forms a singlet state of A ($^1$A*) together with A (eqn 1), and $^1$A*

$$^3A^* + {}^3A^* \rightarrow {}^1A^* + A \qquad (1)$$

finally shows a high-energy UC emission ($h\nu_{UC}$). The least efficient step in the overall TTA-UC process is the bimolecular TTA, which is typically slow because it requires collision of two short-lived triplet excited states $^3$A*. Thus, new approaches that lead to improvement of the efficiencies of the TTA process are important because they are bound to serve as the basis of innovative strategies for the design of potentially important TTA-UC systems.

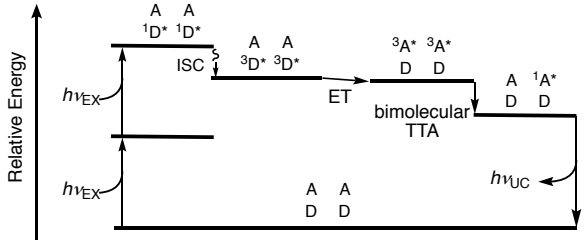


**Fig. 1.** Conventional mechanism for bimolecular TTA-UC.

By using time-resolved spectroscopic studies, several factors that improve the efficiency of singlet fission (SF, eqn 2),[9–15]

$$^1A^* + A \rightarrow (^3A^3A)^* \rightarrow {}^3A^* + {}^3A^* \qquad (2)$$

the reverse of TTA, have been elucidated recently. Importantly, the results of these investigations demonstrate that rapid intramolecular SF takes place in dyads composed of two As and a linker, and that the rate of intramolecular SF and lifetime of the lowest triplet excited ($T_1$) state ($\tau_T$) of the resulting exciton, $^3$A*, is governed by the nature of the linker in which through-space and through-bond electronic coupling between two As.[16–19] Similarly, many TTA-UC systems that operate through "intramolecular TTA" contain dyads of As connected by conjugated[20–22] or nonconjugated[23–26] linkers. It is expected that a rate constant for energy transfer ($k_{ET}$) from $^3$D* to A in these types of dyads would be remarkably large due to the existence of two As in the sole

molecule. However, the effects of linkers, especially on controlling the distance between and relative orientation of the two As, on the efficiency of TTA-UC have not yet been fully explored.

In the investigation described below, we evaluated the photophysical properties and TTA-UC performances of systems composed of the PtOEP donor, and three dyads (DPA–Cn–DPA, n = 1~3, Fig. 2) in which the DPA acceptors have different distances and relative orientations. In one of the three dyads, the two DPA acceptors are linked by a C1 unit of a dimethylmethylene moiety, in the other a C2 unit of a rigid cage structure containing dimethylene moiety serves as the linker,[27] and the last linker is comprised of a C3 unit of an adamantane containing trimethylene moiety.[23] The results of this effort show that systems containing these dyads have larger $\tau_T$ as compared to that of DPA monomer, owing to "Intramolecular Energy Hopping", which reduces the threshold intensity ($I_{TH}$) and leads to efficient TTA-UC.

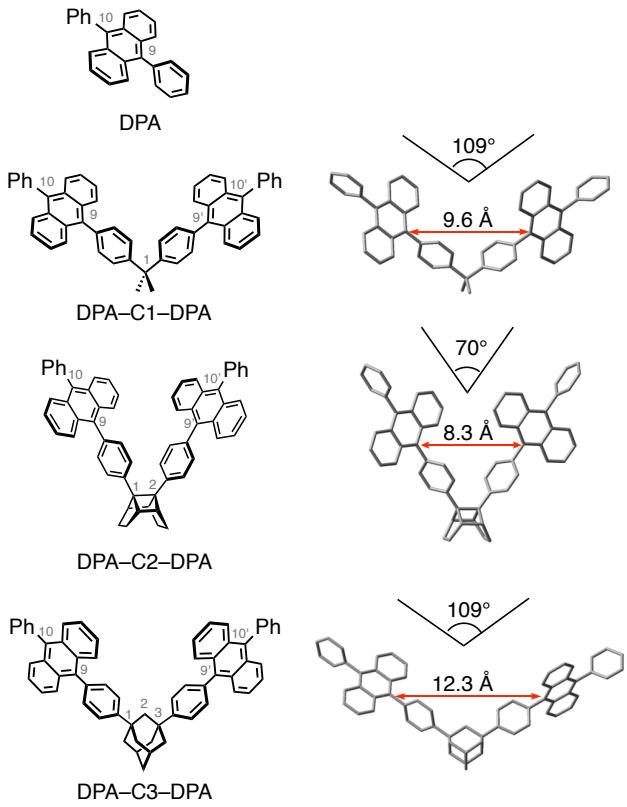


**Fig. 2**. Structures and DFT (B3LYP/6-311G*)-optimized geometries of DPA and DPA–Cn–DPA (n = 1~3).

## Experimental Section

**Preparation of Substrates.** Dyads, DPA–C1–DPA and DPA–C2–DPA, were synthesized by using Suzuki–Miyaura cross-coupling reaction of the corresponding trifrate **1** and bromide **3**,[27] with 10-phenylanthracen-9-yl boronic acid ester **2** or the corresponding boronic acid **4** (Scheme 1). Synthesis of DPA–C3–DPA and PtOEP have been reported previously.[23]

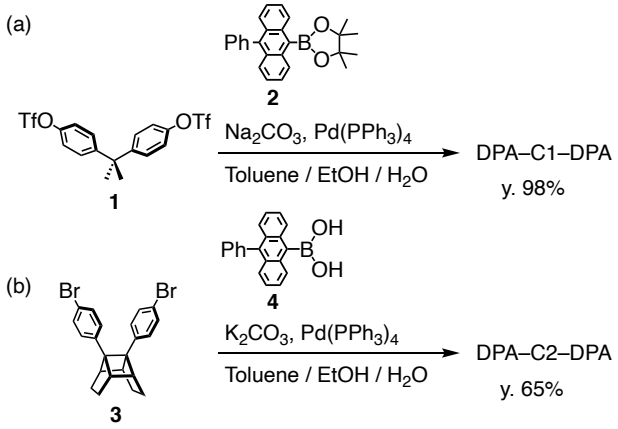


**Scheme 1.** Routes for synthesis of (a) DPA–C1–DPA and (b) DPA–C2–DPA. Tf refers trifluoromethylsulfonyl group.

**Steady-state Spectroscopy.** UV–Vis absorption and photoluminescence spectra were recorded using JASCO V-570 and FP-8500 spectrophotometers, respectively. Absolute fluorescence quantum yields were determined by utilizing the integrating sphere method with a Hamamatsu Photonics C9920-02 under argon. Fluorescence decay profiles were determined under argon by using a HORIBA Jobin Yvon FluoroCube time-correlated single photon counting photometer.

**UC Luminescence.** UC luminescence measurements were made using an Ocean Optics USB4000 multichannel detector upon CW-laser (RGB Photonics, MiniLas Evo, Fiber, 520 nm) excitation. Laser power was controlled by using Ltune software and neutral density filters. The sample solutions in J. Young valve-fused quartz vessels were degassed using three freeze (77 K)–pump (0.1 mmHg)–thaw (room temperature) cycles and then sealed before measurements were made.

**Time-resolved Absorption Spectroscopy.** Measurements were conducted by using a sample solution with an optical density (*OD*) = 0.6 at excitation wavelength in a vessel of 1 cm thickness. The sample solution was degassed by three freeze (77 K)–pump (0.1 mmHg)–thaw (room temperature) cycles. Nanosecond transient absorption was measured on a UNISOKU TSP-1000 setup with THG of YAG laser (355 nm, Spectra Physics Quanta-Ray GC-100, 10 Hz, fwhm = 8 ns, 15 mJ pulse$^{-1}$) or OPA-equipped YAG laser (410–700 nm, Continuum Surelite-3, fwhm = 4 ns, ~10 mJ pulse$^{-1}$) excitation and Xe arc monitoring lamp (150 W).

**Theoretical Calculations.** Density functional theory (DFT) calculations were carried out using Gaussian 09W program[28] using B3LYP functional and 6-311G(d) basis set. Scan calculations were carried out using semiempirical PM5 level of theory. Geometries and orbitals were plotted by using an Avogadro[29] or GaussView[30] program.

## RESULTS AND DISCUSSION

**Dyad Geometries.** In contrast to the two DPA moieties in DPA–C1–DPA, those in dyads DPA–C2–DPA and DPA–C3–DPA have fixed, framework-mandated cisoid geometries. In addition, the distances between and relative orientations of the DPA acceptors in the latter two dyads differ. The results of DFT calculations show

that the respective distances between the $C_9$···$C_{9'}$ positions of the DPA moieties in DPA–C1–DPA, DPA–C2–DPA, and DPA–C3–DPA (Fig. 2) are 9.6, 8.3, and 12.3 Å. The short $C_9$···$C_{9'}$ distance in DPA–C2–DPA is a consequence of the narrow angle (*ca.* 70°) that exist between $C_9$···$C_{10}$ and $C_{9'}$···$C_{10'}$. These distances and angles suggest that relatively strong through-space interaction should take place between the DPA groups in DPA–C2–DPA. It is known that TTA requiring electron exchange is efficient when the distance between the two triplet species $^3$DPA* is shorter than 10 Å.[31,32] Thus, it was expected that efficient intramolecular TTAs would occur in DPA–C1–DPA and DPA–C2–DPA despite the fact that free rotation of the DPA moieties should take place in these dyads (Rotational barriers of a single bond in DPA–Cn are less than 2 kcal mol$^{-1}$ according to the calculation of PM5 level. Fig. S12).

**Photophysical Properties.** DPA in $CH_2Cl_2$ has respective absorption ($\lambda_{AB}$) and fluorescence ($\lambda_{FL}$) maxima at 395 and 413 nm (Fig. 3, black, Table 1), a fluorescence lifetime ($\tau_{FL}$) of 7.7 ns, and a fluorescence quantum yield ($\Phi_{FL}$) of 0.91. Solutions of DPA–Cn–DPA in $CH_2Cl_2$ display absorption bands at 396 nm (Fig. 3, red, blue, and green). Excitation of solutions of DPA–C1–DPA, DPA–C2–DPA, and DPA–C3–DPA at 376 nm leads to intense fluorescence with $\lambda_{FL}$ at 415, 419, and 415 nm, respectively (Fig. 3, red, blue, and green). Although the dyads do not form remarkable intramolecular excimers, DPA–C2–DPA displays a slightly redshifted and broadened fluorescence band, probably as a result of weak through-space excitonic coupling. The values of $\Phi_{FL}$ and $\tau_{FL}$ of the three dyads along with those of DPA are listed in Table 1. Also included in this table are rate constants for fluorescence emission ($k_{FL}$) and nonradiative deactivation ($k_{NR}$) calculated using eqns 3 and 4. The results show that the $\Phi_{FL}$ of DPA–C2–DPA (0.72) is

$$k_{FL} = \Phi_{FL}/\tau_{FL} \qquad (3)$$

$$k_{NR} = (1 - \Phi_{FL})/\tau_{FL} \qquad (4)$$

slightly lower than those of DPA and the other dyads as a result of having a larger $k_{NR}$. The nearly identical $k_{FL}$ values of DPA and the three dyads suggest that through-space and through-bond interactions between two DPA moieties in the lowest singlet excited ($S_1$) states of DPA–Cn–DPA are not remarkable.

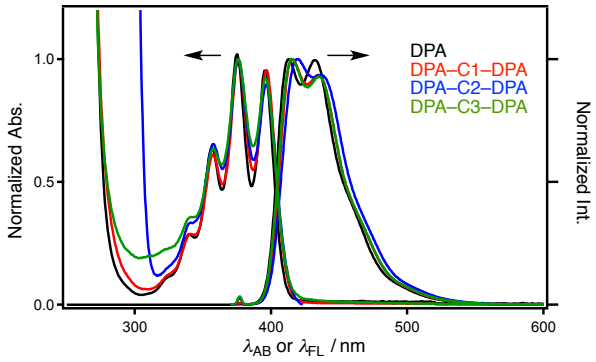


**Fig. 3.** UV–Vis absorption and fluorescence spectra of (black) DPA, (red) DPA–C1–DPA, (blue) DPA–C2–DPA, and (green) DPA–C3–DPA in $CH_2Cl_2$ ($\lambda_{EX}$ = 375 nm).

**Table 1.** Photophysical Properties of DPA and DPA–Cn–DPA in $CH_2Cl_2$

| Compound | $\lambda_{AB}$ / nm | $\lambda_{FL}$ / nm | $\Phi_{FL}$ | $\tau_{FL}$ / ns | $k_{FL}$ / $10^6$ s$^{-1}$ | $k_{NR}$ / $10^6$ s$^{-1}$ |
|---|---|---|---|---|---|---|
| DPA | 375, 395 | 413 | 0.91 | 7.7 | 11.8 | 1.17 |
| DPA–C1–DPA | 376, 396 | 415 | 0.87 | 6.7 | 13.0 | 1.94 |
| DPA–C2–DPA | 376, 396 | 419 | 0.72 | 5.5 | 13.1 | 5.10 |
| DPA–C3–DPA | 376, 396 | 415 | 0.87 | 6.7 | 13.0 | 1.94 |

**TTA-UC Characteristics.** As expected, degassed $CH_2Cl_2$ solutions of dyads DPA–Cn–DPA and PtOEP display TTA-UC luminescence at 435 nm upon excitation at 520 nm (Fig. S2). The $I_{TH}$ value is an important index for evaluating how the system works with the low excitation intensity.[33,34] Consequently, double-logarithmic plot analyses of UC emission intensities ($I_{UC}$) against various excitation intensities ($I_{EX}$) were carried out on degassed $CH_2Cl_2$ solutions containing PtOEP along with DPA or the DPA–Cn–DPA dyads (Fig. 4). In these measurements, the quantum yields for triplet ET process ($\Phi_{ET}$) were adjusted to be 0.98, based on a consideration of ET rate constants ($k_{ET}$, Table S1) and by controlling DPA–Cn–DPA concentrations. The $I_{UC}$ of TTA-UC for DPA–C1–DPA and DPA–C3–DPA are nearly the same as that of the parent DPA. These results clearly show that $I_{UC}$ is governed by concentration of the triplet species with the $^3$DPA* moiety, not by the prepared concentration of the ground state DPA. Employment of Kamada fitting function shown in eqn 5,[35–37]

$$I_{UC} = KI_{EX}\left[1 + \frac{1-\sqrt{1+4I_{EX}/I_{TH}}}{2I_{EX}/I_{TH}}\right] \qquad (5)$$

where $K$ is a proportional constant, provided the respective $I_{TH}$ values of 13, 27, 10, and 28 mW cm$^{-2}$ for DPA, DPA–C1–DPA, DPA–C2–DPA, and DPA–C3–DPA. Importantly, the results demonstrate that dyad DPA–C2–DPA has a low $I_{TH}$ value that is comparable to that of DPA.

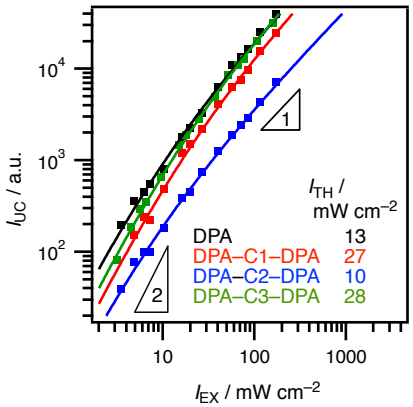


**Fig. 4.** Double-logarithmic plots and fitted curves of $I_{UC}$ at 435 nm against $I_{EX}$ upon the 520-nm excitation of a degassed $CH_2Cl_2$ solution of DPA (black, 0.7 mM), DPA–C1–DPA (red, 0.4 mM), DPA–C2–DPA (blue, 0.5 mM), or DPA–C3–DPA (green, 0.5

mM) containing PtOEP (0.05 mM). Kamada fitting function (eqn 5)[35–37] was employed.

**Triplet Lifetime Analysis.** The $I_{TH}$ value can be related to a rate constant for triplet–triplet annihilation ($k_{TTA}$), $\Phi_{ET}$, and $\tau_T$ by the relationship shown in eqn 6.[5,33] Thus, $\tau_T$ is an essential factor

$$I_{TH} \propto 1 / k_{TTA} \Phi_{ET} \tau_T^2 \qquad (6)$$

controlling $I_{TH}$. Recently, it was reported that covalently-linked dyads of π-conjugated systems have remarkably large $\tau_T$.[11,13,21] To gain further insights into the TTA-UC of the three dyads, $\tau_T$ values of DPA–C1–DPA, DPA–C2–DPA, and DPA–C3–DPA in degassed $CH_2Cl_2$ were determined using PtOEP-sensitized transient absorption analysis. The $\tau_T$ value for $^3$DPA* was determined to be 179 μs by analysis of the 450-nm decay profile (Fig. 5a).[38] Similar measurements gave $\tau_T$ values for DPA–C1–DPA, DPA–C2–DPA, and DPA–C3–DPA of 291, 249, and 224 μs, respectively (Fig. 5b–d). Thus, the $\tau_T$ values of all dyads are larger than that of DPA.[11] If the parent DPA and the three dyads were to have the same $k_{TTA}$ values, the expected $I_{TH}$ values obtained by using $\tau_T$ and eqn 6 for DPA–C1–DPA, DPA–C2–DPA, and DPA–C3–DPA would be 0.38, 0.52, and 0.64 times the $I_{TH}$ value of DPA, respectively. However, the actual $I_{TH}$ values for the corresponding dyads are 2.1, 0.77, and 2.2 times the $I_{TH}$ value of DPA. This finding indicates that the $k_{TTA}$ values of the dyads are different and uniquely dependent on their molecular structure. Because $\Phi_{ET}$ was adjusted to 0.98 in all systems, relative $k_{TTA}$ values can be obtained using eqn 6 (Table 2). Note that the "TTA" discussed here is a not an elementary process, but an overall process that includes association of two $^3$DPA*–Cn–DPA.

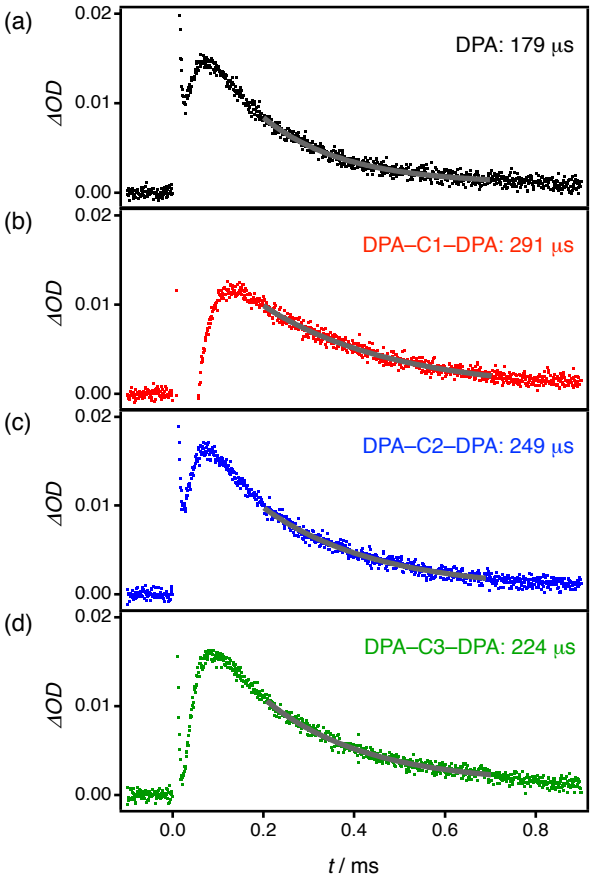


**Fig. 5.** Decay profiles of the absorption of the $^3$DPA* moiety at 450 nm in degassed $CH_2Cl_2$ solution of the parent DPA (a, 0.05 mM) or DPA–C1–DPA (b, 0.05 mM), DPA–C2–DPA (c, 0.05 mM), or DPA–C3–DPA (d, 0.05 mM) containing PtOEP (0.05 mM).

**Table 2.** Parameters Related to TTA-UC of DPA and DPA–Cn–DPA

| Compound | $\theta$ / °[a] | $d$ / Å[a] | $\tau_T$ / μs[b] | $I_{TH}$ / mW cm$^{-2}$ | Relative $k_{TTA}$[c] |
|---|---|---|---|---|---|
| DPA | — | — | 179 | 13 | 1 |
| DPA–C1–DPA | 109 | 9.6 | 291 | 27 | 0.18 |
| DPA–C2–DPA | 70 | 8.3 | 249 | 10 | 0.68 |
| DPA–C3–DPA | 109 | 12.1 | 224 | 28 | 0.29 |

[a] Obtained by using DFT-optimized geometries. [b] Obtained by using degassed $CH_2Cl_2$ solutions containing PtOEP. [c] Determined by using $\tau_T$, $I_{TH}$, and eqn 6 relative to $k_{TTA}$ of DPA.

The large $\tau_T$ values of $^3$DPA* containing dyads can be explained by invoking "Intramolecular Energy Hopping" from $^3$DPA* to the other DPA moiety. Using the generally-accepted explanation,[39–42] nonradiative deactivation of excited triplet species of monomeric systems takes place at the conical intersection (CI) of $T_1$ and the ground ($S_0$) state surfaces (Fig. 6a, pink arrows), and is associated with a molecular motion (e.g., molecular distortion) along with the $T_1$ potential surface. If, as is the case in DPA–Cn–DPA, another DPA moiety exists within close distance, jump from $T_1$ to another triplet $T_1$' energy surface (Fig. 6b, pink arrow) associated with

"Intramolecular Energy Hopping" is possible before reaching CI. Thus, nonradiative deactivation of $^3$DPA*–Cn–DPA is suppressed, as compared with that of the parent $^3$DPA*. This type of phenomenon has been frequently observed for dyads linked by conjugated or nonconjugated tethers.[11,13,21,43] Actually, the longer $\tau_T$ of $^3$DPA*–Cn–DPA were obtained under the heavy-atom-free benzophenone-sensitized conditions (e.g. 623 μs for DPA–C1–DPA, Fig. S4).[44] Thus, the magnitude of elongation of $\tau_T$ is strongly depending on the environment, such as solvent, external heavy atom, temperature, etc.

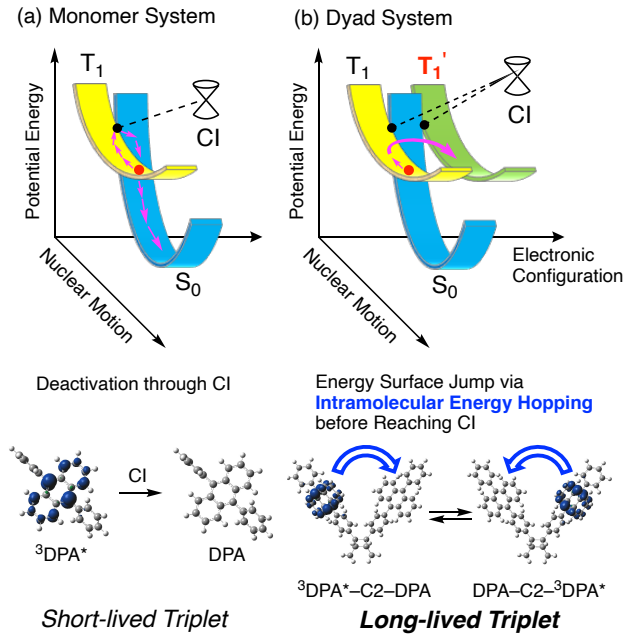


**Fig. 6.** Schematic representations of mechanism for deactivation of $T_1$-excited species of (a) monomer and (b) dyad systems through CI. The elongation of $\tau_T$ of dyad system caused by "Intramolecular Energy Hopping" between two DPA moieties, due to the existence of $T_1$ and $T_1$' surfaces. The spin distribution of $^3$DPA* and $^3$DPA*–C2–DPA are also displayed.

## CONCLUSIONS

In the investigation described above, we examined the TTA-UC behavior of three dyads DPA–Cn–DPA (n = 1~3), in which the DPA moieties are linked by nonconjugated units. Although the fluorescence properties of the dyads are almost identical, their TTA-UC characteristics reflected in $I_{TH}$ values differ greatly. The results of spectroscopic analysis demonstrate that the structures of the dyads affect their $\tau_T$ and $k_{TTA}$. The nonconjugated linkers in these systems effectively elongate $\tau_T$ by suppressing nonradiative deactivation, through "Intramolecular Energy Hopping". It is anticipated that a better dyad orientation would also enable a faster TTA through an intramolecular process, though the analysis of TTA process have not reached to the level that reveals an acceleration of $k_{TTA}$. The original strategy of elongation of $\tau_T$ described in this effort will plays an important role in improving the characteristics of not only TTA-UC systems[45] but also other devices that operate through formation and decay of triplet-excited species[46] such as organic light-emitting diodes[47,48] and organic solar cells.[7,8,49,50]

## ASSOCIATED CONTENT

### Supporting Information

The Supporting Information is available free of charge on the Publications website at DOI: XXXX.

General, Preparation of Substrates, Phosphorescence Quenching Experiments, Raw Data of UC Luminescence Spectrum, Determination of Triplet Lifetime under the Benzophenone-sensitization Conditions, NMR Spectra, and Theoretical Calculations

## AUTHOR INFORMATION


### Corresponding Authors

**Yasunori Matsui** — *Department of Applied Chemistry, Graduate School of Engineering, and The Research Institute for Molecular Electronic Devices (RIMED), Osaka Prefecture University, 1-1 Gakuen-cho, Nakaku, Sakai, Osaka 599-8531, Japan;* orcid.org/0000-0002-7719-0071; Email: matsui@chem.osakafu-u.ac.jp (YM)

**Hiroshi Ikeda** —*Department of Applied Chemistry, Graduate School of Engineering, and The Research Institute for Molecular Electronic Devices (RIMED), Osaka Prefecture University, 1-1 Gakuen-cho, Nakaku, Sakai, Osaka 599-8531, Japan*; orcid.org/0000-0002-8161-2177; Email: ikeda@chem.osakafu-u.ac.jp (HI)

### Authors

**Masaya Kanoh** — *Department of Applied Chemistry, Graduate School of Engineering, Osaka Prefecture University, 1-1 Gakuen-cho, Nakaku, Sakai, Osaka 599-8531, Japan;* orcid.org/0000-0003-1625-573X

**Kiyomasa Honda** — *Department of Applied Chemistry, Graduate School of Engineering, Osaka Prefecture University, 1-1 Gakuen-cho, Nakaku, Sakai, Osaka 599-8531, Japan*

**Yuto Kokita** — *Department of Applied Chemistry, Graduate School of Engineering, Osaka Prefecture University, 1-1 Gakuen-cho, Nakaku, Sakai, Osaka 599-8531, Japan*

**Takuya Ogaki** — *Department of Applied Chemistry, Graduate School of Engineering, and The Research Institute for Molecular Electronic Devices (RIMED), Osaka Prefecture University, 1-1 Gakuen-cho, Nakaku, Sakai, Osaka 599-8531, Japan*; orcid.org/0000-0003-2639-141X

**Eisuke Ohta** — *Department of Applied Chemistry, Graduate School of Engineering, and The Research Institute for Molecular Electronic Devices (RIMED), Osaka Prefecture University, 1-1 Gakuen-cho, Nakaku, Sakai, Osaka 599-8531, Japan*

### Dedication

This paper is dedicated to the memory of Emer. Prof. Toshio Mukai and Emer. Prof. Tsutomu Miyashi at Tohoku University.

## Notes

The authors declare no competing financial interests.

## ACKNOWLEDGEMENT

This work was partially supported by JSPS KAKENHI Grant (Nos. JP24109009, JP23350023, JP18H01967, JP20H02716, JP20K15264, JP19H00888, JP18K14202, JP17H01265, JP17K19105, JP17H06375, JP17H06372, JP16H04097). YM also acknowledges Sasakawa Scientific Research Grant (29-303) and Kansai Research Foundation for Technology Promotion.

## REFERENCES and NOTES

(1) Singh-Rachford, T. N.; Castellano, F. N. Photon Upconversion Based on Sensitized Triplet–Triplet Annihilation. *Coord. Chem. Rev.* **2010**, *254*, 2560–2573.

(2) Zhou, J.; Liu, Q.; Feng, W.; Sun, Y.; Li, F. Upconversion Luminescent Materials: Advances and Applications. *Chem. Rev.* **2015**, *115*, 395–465.

(3) Haruki, R.; Sasaki, Y.; Masutani, K.; Yanai, N.; Kimizuka, N. Leaping across the Visible Range: Near-Infrared-to-Violet Photon Upconversion Employing a Silyl-Substituted Anthracene. *Chem. Commun.* **2020**, *56*, 7017–7020.

(4) Pristash, S. R.; Corp, K. L.; Rabe, E. J.; Schlenker, C. W. Heavy-Atom-Free Red-to-Yellow Photon Upconversion in a Thiosquaraine Composite. *ACS Appl. Energy Mater.* **2020**, *3*, 19–28.

(5) Monguzzi, A.; Tubino, R.; Hoseinkhani, S.; Campione, M.; Meinardi, F. Low Power, Non-Coherent Sensitized Photon Up-Conversion: Modelling and Perspectives. *Phys. Chem. Chem. Phys.* **2012**, *14*, 4322–4332.

(6) Sasaki, Y.; Amemori, S.; Kouno, H.; Yanai, N.; Kimizuka, N. Near Infrared-to-Blue Photon Upconversion by Exploiting Direct S-T Absorption of a Molecular Sensitizer. *J. Mater. Chem. C* **2017**, *5*, 5063–5067.

(7) Dilbeck, T.; Hanson, K. Molecular Photon Upconversion Solar Cells Using Multilayer Assemblies: Progress and Prospects. *J. Phys. Chem. Lett.* **2018**, *9*, 5810–5821.

(8) Shang, Y.; Hao, S.; Yang, C.; Chen, G. Enhancing Solar Cell Efficiency Using Photon Upconversion Materials. *Nanomaterials* **2015**, *5*, 1782–1809.

(9) Smith, M. B.; Michl, J. Singlet Fission. *Chem. Rev.* **2010**, *110*, 6891–6936.

(10) Sanders, S. N.; Kumarasamy, E.; Pun, A. B.; Steigerwald, M. L.; Sfeir, M. Y.; Campos, L. M. Intramolecular Singlet Fission in Oligoacene Heterodimers. *Angew. Chem. Int. Ed.* **2016**, *55*, 3373–3377.

(11) Nakamura, S.; Sakai, H.; Nagashima, H.; Kobori, Y.; Tkachenko, N. V; Hasobe, T. Quantitative Sequential Photoenergy Conversion Process from Singlet Fission to Intermolecular Two-Electron Transfers Utilizing Tetracene Dimer. *ACS Energy Lett.* **2019**, *4*, 26–31.

(12) Bhattacharyya, K.; Dey, D.; Datta, A. Intramolecular Singlet Fission in Quinoidal Dihydrothiophene. *J. Phys. Chem. C* **2019**, *123*, 4749–4754.

(13) Matsui, Y.; Kawaoka, S.; Nagashima, H.; Nakagawa, T.; Okamura, N.; Ogaki, T.; Ohta, E.; Akimoto, S.; Sato-Tomita, A.; Yagi, S.; Kobori, Y.; Ikeda, H. Exergonic Intramolecular Singlet Fission of an Adamantane-Linked Tetracene Dyad via Twin Quintet Multiexcitons. *J. Phys. Chem. C* **2019**, *123*, 18813–18823.

(14) Kumarasamy, E.; Sanders, S. N.; Tayebjee, M. J. Y.; Asadpoordarvish, A.; Hele, T. J. H.; Fuemmeler, E. G.; Pun, A. B.; Yablon, L. M.; Low, J. Z.; Paley, D. W.; Dean, J. C.; Choi, B.; Scholes, G. D.; Steigerwald, M. L.; Ananth, N.; McCamey, D. R.; Sfeir, M. Y.; Campos, L. M. Tuning Singlet Fission in π-Bridge-π Chromophores. *J. Am. Chem. Soc.* **2017**, *139*, 12488–12494.

(15) Smith, M. B.; Michl, J. Recent Advances in Singlet Fission. *Annu. Rev. Phys. Chem.* **2013**, *64*, 361–386.

(16) Korovina, N. V; Pompetti, N. F.; Johnson, J. C. Lessons from Intramolecular Singlet Fission with Covalently Bound Chromophores. *J. Chem. Phys.* **2020**, *152*, 40904.

(17) Basel, B. S.; Zirzlmeier, J.; Hetzer, C.; Reddy, S. R.; Phelan, B. T.; Krzyaniak, M. D.; Volland, M. K.; Coto, P. B.; Young, R. M.; Clark, T.; Thoss, M.; Tykwinski, R. R.; Wasielewski, M. R.; Guldi, D. M. Evidence for Charge-Transfer Mediation in the Primary Events of Singlet Fission in a Weakly Coupled Pentacene Dimer. *Chem* **2018**, *4*, 1092–1111.

(18) Korovina, N. V.; Joy, J.; Feng, X.; Feltenberger, C.; Krylov, A. I.; Bradforth, S. E.; Thompson, M. E. Linker-Dependent Singlet Fission in Tetracene Dimers. *J. Am. Chem. Soc.* **2018**, *140*, 10179–10190.

(19) Hetzer, C.; Guldi, D. M.; Tykwinski, R. R. Pentacene Dimers as a Critical Tool for the Investigation of Intramolecular Singlet Fission. *Chem. –Eur. J.* **2018**, *24*, 8245–8257.

(20) Dzebo, D.; Börjesson, K.; Gray, V.; Moth-Poulsen, K.; Albinsson, B. Intramolecular Triplet–Triplet Annihilation Upconversion in 9,10-Diphenylanthracene Oligomers and Dendrimers. *J. Phys. Chem. C* **2016**, *120*, 23397–23406.

(21) Pun, A. B.; Sanders, S. N.; Sfeir, M. Y.; Campos, L. M.; Congreve, D. N. Annihilator Dimers Enhance Triplet Fusion Upconversion. *Chem. Sci.* **2019**, *10*, 3969–3975.

(22) Gao, C.; Prasad, S. K. K.; Zhang, B.; Dvořák, M.; Tayebjee, M. J. Y.; McCamey, D. R.; Schmidt, T. W.; Smith, T. A.; Wong, W. W. H. Intramolecular Versus Intermolecular Triplet Fusion in Multichromophoric Photochemical Upconversion. *J. Phys. Chem. C* **2019**, *123*, 20181–20187.

(23) Matsui, Y.; Kanoh, M.; Ohta, E.; Ogaki, T.; Ikeda, H. Triplet–Triplet Annihilation-Photon Upconversion Employing an Adamantane-Linked Diphenylanthracene Dyad Strategy. *J. Photochem. Photobiol. A Chem.* **2020**, *387*, 112107.

(24) Tilley, A. J.; Robotham, B. E.; Steer, R. P.; Ghiggino, K. P. Sensitized Non-Coherent Photon Upconversion by Intramolecular Triplet–Triplet Annihilation in a Diphenylanthracene Pendant Polymer. *Chem. Phys. Lett.* **2015**, *618*, 198–202.

(25) Ribas, M. R.; Steer, R. P.; Rüther, R. Photophysical Properties of New Bis-Perylene Dyads for Potential Upconversion Use. *Chem. Phys. Lett.* **2014**, *605–606*, 126–130.

(26) Yu, S.; Zeng, Y.; Chen, J.; Yu, T.; Zhang, X.; Yang, G.; Li, Y. Intramolecular Triplet–Triplet Energy Transfer Enhanced Triplet–Triplet Annihilation Upconversion with a Short-

Lived Triplet State Platinum(II) Terpyridyl Acetylide Photosensitizer. *RSC Adv.* **2015**, *5*, 70640–70648.

(27) Kuramoto, Y.; Matsui, Y.; Ohta, E.; Sato, H.; Ikeda, H. Unexpected Formation of a Phenonium Ion-Containing Salt by Single Electron-Transfer Oxidation of a Cage Compound Possessing Triphenylamine Moieties. *Tetrahedron Lett.* **2014**, *55*, 4366–4369.

(28) Frisch, M. J.; Trucks, G. W.; Schlegel, H. B.; Scuseria, G. E.; Robb, M. A.; Cheeseman, J. R.; Scalmani, G.; Barone, V.; Mennucci, B.; Petersson, G. A.; Nakatsuji, H.; Caricato, M.; Li, X.; Hratchian, H. P.; Izmaylov, A. F.; Bloino, J.; Zheng, G.; Sonnenberg, J. L.; Hada, M.; Ehara, M.; Toyota, K.; Fukuda, R.; Hasegawa, J.; Ishida, M.; Nakajima, T.; Honda, Y.; Kitao, O.; Nakai, H.; Vreven, T.; Montgomery Jr., J. A.; Peralta, J. E.; Ogliaro, F.; Bearpark, M.; Heyd, J. J.; Brothers, E.; Kudin, K. N.; Staroverov, V. N.; Kobayashi, R.; Normand, J.; Raghavachari, K.; Rendell, A.; Burant, J. C.; Iyengar, S. S.; Tomasi, J.; Cossi, M.; Rega, N.; Millam, J. M.; Klene, M.; Knox, J. E.; Cross, J. B.; Bakken, V.; Adamo, C.; Jaramillo, J.; Gomperts, R.; Stratmann, R. E.; Yazyev, O.; Austin, A. J.; Cammi, R.; Pomelli, C.; Ochterski, J. W.; Martin, R. L.; Morokuma, K.; Zakrzewski, V. G.; Voth, G. A.; Salvador, P.; Dannenberg, J. J.; Dapprich, S.; Daniels, A. D.; Farkas, Ö.; Foresman, J. B.; Ortiz, J. V; Cioslowski, J.; Fox, D. J. *Gaussian 09*; 2009.

(29) Hanwell, M. D.; Curtis, D. E.; Lonie, D. C.; Vandermeersch, T.; Zurek, E.; Hutchison, G. R. Avogadro: An Advanced Semantic Chemical Editor, Visualization, and Analysis Platform. *J. Cheminform.* **2012**, *4*, 17.

(30) Dennington, R.; Keith, T.; Millam, J. Gaussview, Version 5. *Semichem Inc., Shawnee Mission, KS*. Semichem Inc 2016.

(31) Sato, R.; Kitoh-Nishioka, H.; Kamada, K.; Mizokuro, T.; Kobayashi, K.; Shigeta, Y. Does Inactive Alkyl Chain Enhance Triplet-Triplet Annihilation of 9,10-Diphenylanthracene Derivatives? *J. Phys. Chem. C* **2018**, *122*, 5334–5340.

(32) Sato, R.; Kitoh-Nishioka, H.; Kamada, K.; Mizokuro, T.; Kobayashi, K.; Shigeta, Y. Synergetic Effects of Triplet–Triplet Annihilation and Directional Triplet Exciton Migration in Organic Crystals for Photon Upconversion. *J. Phys. Chem. Lett.* **2018**, *9*, 6638–6643.

(33) Monguzzi, A.; Mezyk, J.; Scotognella, F.; Tubino, R.; Meinardi, F. Upconversion-Induced Fluorescence in Multicomponent Systems: Steady-State Excitation Power Threshold. *Phys. Rev. B* **2008**, *78*, 195112.

(34) Schmidt, T. W.; Castellano, F. N. Photochemical Upconversion: The Primacy of Kinetics. *J. Phys. Chem. Lett.* **2014**, *5*, 4062–4072.

(35) Kamada, K.; Sakagami, Y.; Mizokuro, T.; Fujiwara, Y.; Kobayashi, K.; Narushima, K.; Hirata, S.; Vacha, M. Efficient Triplet-Triplet Annihilation Upconversion in Binary Crystalline Solids Fabricated: Via Solution Casting and Operated in Air. *Mater. Horiz.* **2017**, *4*, 83–87.

(36) Abulikemu, A.; Sakagami, Y.; Heck, C.; Kamada, K.; Sotome, H.; Miyasaka, H.; Kuzuhara, D.; Yamada, H. Solid-State, Near-Infrared to Visible Photon Upconversion via Triplet-Triplet Annihilation of a Binary System Fabricated by Solution Casting. *ACS Appl. Mater. Interfaces* **2019**, *11*, 20812–20819.

(37) Mori, T.; Mori, T.; Fujii, A.; Saito, A.; Saomoto, H.; Kamada, K. Effect of Crystallinity in Stretched PVA Films on Triplet–Triplet Annihilation Photon Upconversion. *ACS Appl. Polym. Mater.* **2020**, *2*, 1422–1428.

(38) Aulin, Y. V.; van Sebille, M.; Moes, M.; Grozema, F. C. Photochemical Upconversion in Metal-Based Octaethyl Porphyrin–Diphenylanthracene Systems. *RSC Adv.* **2015**, *5*, 107896–107903.

(39) Turro, N. J.; Ramamurthy, V.; Scaiano, J. C. *Principles of Molecular Photochemistry: An Introduction*; University Science Books, 2009.

(40) Suzuki, S.; Sasaki, S.; Sairi, A. S.; Iwai, R.; Tang, B. Z.; Konishi, G. Principles of Aggregation-Induced Emission: Design of Deactivation Pathways for Advanced AIEgens and Applications. *Angew. Chem. Int. Ed.* **2020**, *59*, 9856–9867.

(41) Harabuchi, Y.; Taketsugu, T.; Maeda, S. Exploration of Minimum Energy Conical Intersection Structures of Small Polycyclic Aromatic Hydrocarbons: Toward an Understanding of the Size Dependence of Fluorescence Quantum Yields. *Phys. Chem. Chem. Phys.* **2015**, *17*, 22561–22565.

(42) Maeda, S.; Taketsugu, T.; Ohno, K.; Morokuma, K. From Roaming Atoms to Hopping Surfaces: Mapping Out Global Reaction Routes in Photochemistry. *J. Am. Chem. Soc.* **2015**, *137*, 3433–3445.

(43) Sakuma, T.; Sakai, H.; Araki, Y.; Mori, T.; Wada, T.; Tkachenko, N. V.; Hasobe, T. Long-Lived Triplet Excited States of Bent-Shaped Pentacene Dimers by Intramolecular Singlet Fission. *J. Phys. Chem. A* **2016**, *120*, 1867–1875.

(44) This result indicates hat the development of heavy-atom free donors is effective to reduce the threshold intensity.

(45) Tokunaga, A.; Uriarte, L. M.; Mutoh, K.; Fron, E.; Hofkens, J.; Sliwa, M.; Abe, J. Photochromic Reaction by Red Light via Triplet Fusion Upconversion. *J. Am. Chem. Soc.* **2019**, *141*, 17744–17753.

(46) Sasikumar, D.; John, A. T.; Sunny, J.; Hariharan, M. Access to the Triplet Excited States of Organic Chromophores. *Chem. Soc. Rev.* **2020**, *49*, 6122–6140.

(47) Graf von Reventlow, L.; Matthias Bremer, A.; Ebenhoch, B.; Martina Gerken, A.; Schmidt, T. W.; Colsmann, A. An Add-on Organic Green-to-Blue Photon-Upconversion Layer for Organic Light Emitting Diodes. *J. Mater. Chem. C* **2018**, *6*, 3845–3848.

(48) Ieuji, R.; Goushi, K.; Adachi, C. Triplet–Triplet Upconversion Enhanced by Spin–Orbit Coupling in Organic Light-Emitting Diodes. *Nat. Commun.* **2019**, *10*, 5283.

(49) Paci, I.; Johnson, J. C.; Chen, X.; Rana, G.; Popović, D.; David, D. E.; Nozik, A. J.; Ratner, M. A.; Michl, J. Singlet Fission for Dye-Sensitized Solar Cells: Can a Suitable Sensitizer Be Found? *J. Am. Chem. Soc.* **2006**, *128*, 16546–16553.

(50) Kinoshita, M.; Sasaki, Y.; Amemori, S.; Harada, N.; Hu, Z.; Liu, Z.; Ono, L. K.; Qi, Y.; Yanai, N.; Kimizuka, N. Photon Upconverting Solid Films with Improved Efficiency for Endowing Perovskite Solar Cells with Near-Infrared Sensitivity. *ChemPhotoChem* **2020**, *4*, 5271–5278.

(EOF)